In vivo microscopy reveals the impact of *Pseudomonas aeruginosa* social interactions on host colonization

Chiara Rezzoagli[1*], Elisa T. Granato[2], Rolf Kümmerli[1*]

[1]Department of Plant and Microbial Biology, University of Zurich, Zurich, Switzerland

[2]Department of Zoology, University of Oxford, Oxford, United Kingdom

* Corresponding authors:

Chiara Rezzoagli or Rolf Kümmerli, Department of Plant and Microbial Biology, University of Zurich, Winterthurerstrasse 190, 8057 Zurich, Switzerland.

Email: chiara.rezzoagli@uzh.ch (CR), rolf.kuemmerli@uzh.ch (RK).

Phone: +41 44 635 48 01.

Abstract

Pathogenic bacteria engage in social interactions to colonize hosts, which include quorum-sensing-mediated communication and the secretion of virulence factors that can be shared as “public goods” between individuals. While in-vitro studies demonstrated that cooperative individuals can be displaced by “cheating” mutants freeriding on social acts, we know little about social interactions in infections. Here, we developed a live imaging system to track virulence factor expression and social strain interactions in the human pathogen *Pseudomonas aeruginosa* colonizing the gut of *Caenorhabditis elegans*. We found that shareable siderophores and quorum-sensing systems are expressed during infections, affect host gut colonization, and benefit non-producers. However, non-producers were unable to cheat and outcompete producers, probably due to the spatial segregation of strains within the gut. Our results shed new light on bacterial social interactions in infections and reveal potential limits of therapeutic approaches that aim to capitalize on social dynamics between strains for infection control.

Introduction

During infections, pathogenic bacteria secrete a wide range of extracellular virulence factors in order to colonize and grow inside the host (Rahme et al., 1995; Wu et al., 2008; Balasubramanian et al., 2013). Secreted molecules include siderophores for iron scavenging, signaling molecules for quorum sensing (QS), toxins to attack host cells, and matrix compounds for biofilm formation (Diggle et al., 2007; West et al., 2007; Henkel et al., 2010; Flemming et al., 2016; Granato et al., 2016). In-vitro studies have shown that extracellular virulence factors can be shared as “public goods” between cells, and thereby benefit individuals other than the producing cell (Köhler et al., 2009; Raymond et al., 2012; Harrison, 2013). There has been enormous interest in understanding how this form of bacterial cooperation can be evolutionarily stable, because secreted public goods can be exploited by non-cooperative mutants called “cheats”, which do not engage in cooperation yet still benefit from the molecules produced by others (Griffin et al., 2004; Diggle et al., 2007; West et al., 2007; Ross-Gillespie et al., 2007; Sandoz et al., 2007; Kümmerli et al., 2009a, 2015; Popat et al., 2012; Ghoul et al., 2014; O’Brien et al., 2017; Özkaya et al., 2018).

There is increasing evidence that social interactions and cooperator-cheat dynamics might also matter within hosts (West and Buckling, 2003; Buckling and Brockhurst, 2008; Harrison, 2013; Leggett et al., 2014). For instance, in a set of controlled infection experiments, it was shown that engineered non-producers, deficient for the production of specific virulence factors, can outcompete producers and thereby reduce virulence (Harrison et al., 2006;

Rumbaugh et al., 2009, 2012; Pollitt et al., 2014), but there are also cases where the success of non-producers was compromised (Zhou et al., 2014; Harrison et al., 2017). Other studies have followed chronic human infections within patients over time and reported that virulence-factor-negative mutants emerge and spread, with the mutational patterns suggesting cooperator-cheat dynamics (Köhler et al., 2009; Andersen et al., 2015, 2018). These findings spurred ideas of how social interactions within hosts could be manipulated for therapeutic purposes (Brown et al., 2009; Allen et al., 2014; Leggett et al., 2014). Suggested approaches include (i) the induction of cooperator-cheat dynamics to steer infections towards lower virulence (Köhler et al., 2009; Granato et al., 2018), (ii) the introduction of less virulent strains with medically beneficial alleles into established infections (Brown et al., 2009), and (iii) the specific targeting of secreted virulence factors to control infections (Clatworthy et al., 2007; Rasko and Sperandio, 2010) and to constrain the evolution of resistance (André and Godelle, 2005; Pepper, 2012; Allen et al., 2014; Rezzoagli et al., 2018).

However, all of these approaches explicitly rely on the assumption that the social traits of interest are: (i) expressed inside hosts; (ii) important for host colonization; (iii) exploitable; and (iv) induce cooperator-cheat dynamics as observed in vitro (Harrison, 2013) – assumptions that have not yet been tested in real time inside living hosts. Here, we explicitly test the importance of bacterial social interactions within hosts by using in-vivo fluorescence microscopy to monitor bacterial virulence factor production, host colonization and strain interactions in a model system, which consist of the opportunistic

pathogen *Pseudomonas aeruginosa* infecting the nematode *Caenorhabditis elegans* (Tan and Ausubel, 2000; Ewbank, 2002; Papaioannou et al., 2013; Utari and Quax, 2013).

C. elegans naturally preys on bacteria (Félix and Braendle, 2010). While most bacteria are killed during ingestion, a small fraction of cells survives (Portal-Celhay et al., 2012), which can, in the case of pathogenic bacteria, establish an infection in the gut (Tan et al., 1999). *P. aeruginosa* deploys an arsenal of virulence factors that facilitate successful host colonization (Nadal Jimenez et al., 2012). For example, the two siderophores pyoverdine and pyochelin scavenge host-bound iron during acute infections to enable pathogen growth (Meyer et al., 1996; Takase et al., 2000; Cornelis and Dingemans, 2013; Parrow et al., 2013; Becker and Skaar, 2014; Granato et al., 2016). *P. aeruginosa* further secretes the protease elastase, the toxin pyocyanin, and rhamnolipid biosurfactants to attack host tissue (Smith and Iglewski, 2003; Alibaud et al., 2008; Köhler et al., 2009; Rumbaugh et al., 2009; Zaborin et al., 2009). Production of these latter virulence factors only occurs at high cell densities and is controlled by the Las and the Rhl quorum sensing (QS) systems (Lee and Zhang, 2015). Because both the QS-regulon and siderophores were shown to be involved in *C. elegans* killing (Mahajan-Miklos et al., 1999; Tan et al., 1999; Papaioannou et al., 2009; Zaborin et al., 2009; Cezairliyan et al., 2013; Kirienko et al., 2013; Zhu et al., 2015), we used them as focal traits for our study.

To tackle our questions, we first conducted experiments with fluorescently tagged *P. aeruginosa* bacteria (PAO1) to follow infection dynamics from first uptake, through feeding and up to a progressed state of gut infection. We then constructed promoter gene fusions for genes involved in the synthesis of the two siderophores (pyoverdine and pyochelin) and the two QS-regulators (LasR and RhlR) to track in vivo virulence factor gene expression during host colonization. Subsequently, we used single and double mutant strains deficient for virulence factors to determine whether they show compromised colonization abilities. And most crucially, we followed mixed infections of wildtype and mutants over time to determine the extent of strain co-localization in the gut, and to test whether secreted virulence factors are indeed exploitable by non-producers in the host.

Results

PAO1 colonization dynamics in the *C. elegans* gut

For all our infection experiments, we followed the protocol depicted in Figure 1A-C. We first exposed worms to *P. aeruginosa* for 24 hours on a nutrient plate. Subsequently, worms were removed, washed, and treated with antibiotics to kill external bacteria. We then imaged infected worms under the microscope at different time points and quantified bacterial density and gene expression profiles using fluorescent mCherry markers. We first confirmed that mCherry fluorescence is a suitable proxy for the number of live bacteria in *C. elegans*, by comparing the fluorescence intensities in whole worms (Figure 1B) to the number of live bacteria recovered from the worms' gut. We found that fluorescence intensity values positively correlated with the bacterial

load inside the nematodes, both immediately after recovering the worms from the exposure plates and at 6 hours post exposure (hpe; Supplementary Figure S1, Pearson correlation coefficient at 0 hpe: $r = 0.49$, $t_{28} = 3.02$, $p = 0.0053$; at 6 hpe: $r = 0.713$, $t_{23} = 4.88$, $p < 0.0001$). As our goal was to image infections in living hosts, we further confirmed that worms stayed alive during the observation period (Supplementary Figure S2).

When using fluorescence intensity to follow host colonization by the wildtype PAO1-mCherry strain over time, we observed that immediately after removal from the exposure plate, worms carried large amounts of bacteria in their gut (Figure 1D). Subsequently, bacterial load significantly declined when the worms were kept in buffer for 6 hours (ANOVA: $t_{391} = -8.55$, $p < 0.001$) and remained constant for the next 24 hours ($t_{391} = 0.61$, $p = 0.529$). This pattern suggests that a large number of bacteria are taken up during the feeding phase, of which a high proportion is shed afterwards, leaving behind a fraction of live bacteria that establishes an infection and colonizes the worm gut.

PAO1 expresses siderophore biosynthesis genes and QS regulators in the host

We then examined whether genes involved in the synthesis of pyoverdine (*pvdA*) and pyochelin (*pchEF*), and the genes *lasR* and *rhlR* encoding two major QS-regulators, are expressed inside hosts. Worms were exposed to four different PAO1 wildtype strains each carrying a specific promoter-mCherry gene reporter fusion. Imaging after the initial uptake phase (0 hpe) revealed that, with the exception of *pchEF*, all genes were significantly expressed in the

host (Figure 2; ANOVA, comparisons to the non-fluorescent control, for *pvdA*: $t_{754} = 4.23$, $p < 0.001$; for *pchEF*: $t_{754} = 0.74$, $p = 0.461$; for *lasR*: $t_{754} = 2.96$, $p = 0.003$; for *rhlR*: $t_{754} = 10.37$, $p < 0.001$). Although fluorescence intensity declined over time (linear model, $F_{1,1795} = 48.98$, $p < 0.001$), we observed that apart from *pchEF*, all genes were still significantly expressed at 30 hpe (Figure 2; ANOVA, for *pvdA*: $t_{754} = 4.87$, $p < 0.001$; for *pchEF*: $t_{754} = 0.684$, $p = 0.461$; for *lasR*: $t_{754} = 3.01$, $p = 0.003$; for *rhlR*: $t_{754} = 16.68$, $p < 0.001$). These results suggest that the siderophore pyoverdine and QS-regulated traits may be important for both initial uptake and subsequent colonisation of the host.

Regulatory links between social traits operate inside the host

We know that regulatory links exist between the virulence traits studied here. While pyoverdine synthesis suppresses pyochelin production under stringent iron limitation (Dumas et al., 2013), the Las-QS system positively activates the Rhl-QS system (Lee and Zhang, 2015). To test whether these links operate inside the nematode host, we measured gene expression of each trait in the negative background of the co-regulated trait (Figure 3). For *pvdA*, we observed significant gene expression levels in both the wildtype PAO1 and the pyochelin-deficient PAO1 Δ*pchEF* strain (Figure 3A), albeit the overall expression was slightly reduced in PAO1 Δ*pchEF* (t-test, $t_{253} = 8.67$, $p < 0.001$). For *pchEF*, expression patterns confirm the suppressive nature of pyoverdine: the pyochelin synthesis gene was not expressed in the wildtype but significantly upregulated in the pyoverdine-deficient PAO1 Δ*pvdD* strain (Figure 3B; $t_{296} = -19.68$, $p < 0.001$). For *lasR*, we found that gene expression was not significantly different in the wildtype PAO1 compared to the Rhl-

180 negative mutant PAO1 Δ*rhlR*, confirming that the Las-QS system is at the top of the hierarchy and not influenced by the Rhl-system (Figure 3C; t_{211} = -1.50, 182 p = 0.136,). Conversely, the expression of *rhlR* was strongly dependent on a functional Las-system, and therefore only expressed in the wildtype PAO1, but 184 repressed in the Las-negative mutant PAO1 Δ*lasR* (Figure 3D; t_{156} = 19.04, p < 0.001,). Taken together, these analyses show that (i) iron-limitation is strong 186 in *C. elegans* as the wildtype primarily invests in the more potent siderophore pyoverdine; (ii) pyochelin can potentially have compensatory effects when 188 pyoverdine is lacking; and (iii) the loss of the Las-system leads to the concomitant collapse of the Rhl-system.

190

Virulence-factor-negative mutants show trait-specific deficiencies in host 192 **colonization**

To examine whether the ability to produce shared virulence factors is 194 important for initial bacterial uptake and host colonization, we exposed *C. elegans* to five isogenic mutants of the PAO1-mCherry strain, either 196 impaired in the production of pyoverdine (Δ*pvdD*), pyochelin (Δ*pchEF*), both siderophores (Δ*pvdD*Δ*pchEF*), the QS receptor LasR (Δ*lasR*), or the QS 198 receptor RhlR (Δ*rhlR*). When analyzing bacterial load after the feeding phase, we observed that the wildtype and all three siderophores mutants were equally 200 abundant inside hosts, whereas bacterial load was significantly reduced for the two QS-mutants compared to the wildtype (Figure 4A; ANOVA, significant 202 variation among strains $F_{5,736}$ = 10.50, p < 0.001; post-hoc Tukey test for multiple comparisons: p > 0.05 for all siderophore mutants, p = 0.021 for 204 PAO1 *ΔlasR*, p < 0.001 for PAO1 *ΔrhlR*).

Consistent with our findings for PAO1 wildtype colonization (Figure 1D), we observed that the bacterial load of all strains declined at 6 hpe (Supplementary Figure S3) and 30 hpe (Figure 4B) following worm removal from the exposure plates. This decline was significantly more pronounced for the double-siderophore knockout PAO1 *ΔpvdDΔpchEF* than for the wildtype (Figure 4B; ANOVA, post-hoc Tukey test $p < 0.001$). In contrast, we found that the mutants deficient in pyochelin (PAO1 *ΔpchEF*) and RhlR (PAO1 *ΔrhlR*) production showed a significantly higher ability to remain in the host than the wildtype (Figure 4B; ANOVA, post-hoc Tukey test $p < 0.001$ for both strains). Taken together, our findings suggest that the two siderophores can complement each other, and that only the siderophore double mutant and the LasR-deficient strain have an overall disadvantage in colonizing worms.

Mixed communities are formed inside hosts, but exploitation of social traits is constrained

Given our findings on colonization deficiencies, we reasoned that the siderophore-double mutant (PAO1 *ΔpvdDΔpchEF*) and the Las-deficient mutant (PAO1 *ΔlasR*) could act as cheats and benefit from the exploitation of virulence factors produced by the wildtype in mixed infections. To test this hypothesis, we first competed the wildtype PAO1-mcherry against the untagged PAO1 strain in the host, and found that the mCherry tag had a small but negative effect on PAO1 fitness (Figure 5A; one sample t-test, $t_{24} = -4.12$, $p < 0.001$). We then competed the wildtype PAO1-mcherry against the two putative cheats in the host and found that neither of the two mutants could

gain a significant fitness advantage over the wildtype, but also did not lose out (Figure 5A; ANOVA, $F_{2,70}$ = 0.517, p = 0.598). These results indicate that mutants, deficient for virulence factor production and compromised in host colonization, can indeed benefit from the presence of the wildtype producer, but not to an extent that would allow them to increase in frequency and displace producers.

Since the wildtype alone was able to maintain higher bacterial loads in the worms compared to the two mutants (Figure 4B), we hypothesized that frequencies of the wildtype in mixed infections should positively correlate with the total bacterial load in the gut. Consistent with our predictions, we found that at 6 hpe, the frequency of wildtype PAO1-mCherry positively correlated with bacterial load in mixed infections with the two non-producers, but not in the control mixed infections with the untagged wildtype (Pearson correlation coefficient, r = 0.54, t_{17} = 2.67, p = 0.016 (PAO1 *ΔlasR),* r = 0.40, t_{17} = 1.77, p = 0.031 (PAO1 *ΔpvdDΔpchEF*); r = 0.12, t_{17} = 0.47, p = 0.639 (PAO1)). These correlations disappeared at the later colonization stage (48 hpe; Pearson correlation coefficient r < 0 for all strains).

Spatial distribution and strain co-localization varies substantially across host individuals

Previous in-vitro studies have shown that the spatial proximity of cells is crucial for the efficient sharing of secreted compounds (Kümmerli et al., 2009a; Van Gestel et al., 2014; Scholz and Greenberg, 2015; Weigert and Kümmerli, 2017). To assess spatial proximity of co-infecting strains in vivo, we

imaged worms exposed to a mix of two strains tagged with either GFP or mCherry and determined strain co-localization in the host (Figure 6). We found that all worms were colonized by both strains, but co-localization within the worm varied greatly across individuals. Specifically, the correlation between mCherry and GFP fluorescence from tail to head ranged from almost perfect co-localization in some worms (Figure 6A; r = 1,) to near complete spatial segregation in other individuals (Figure 6B; r < 0,). Similar co-localization patterns emerged for all three strain combinations tested, highlighting that the type of competitor did not influence the degree of strain co-localization in the host gut (Figure 6C; ANOVA, $F_{2,102} = 2.17$, $p = 0.119$). Important to note in this context is that we calculated co-localization based on a 2-dimensional projection of a 3-dimensional organ (i.e. the gut), which might overestimate the level of co-localization along the z-axis.

Discussion

We developed a live imaging system that allows us to track host colonization by pathogenic bacteria (*P. aeruginosa*) and the expression of bacterial virulence factors inside hosts (*C. elegans*). We used this system to focus on the role of secreted virulence factors, which can be shared as public goods between bacterial cells, and examined competitive dynamics between virulence factor producing and non-producing strains in the host. We found that the two shareable siderophores pyoverdine and pyochelin and the social Las and Rhl quorum-sensing systems: (i) are expressed inside the host, (ii) affect the ability to colonize and reside within the nematodes; (iii) allow non-producers to benefit from virulence factors secreted by producers in mixed

infections; but (iv) do not allow non-producers to cheat and outcompete producers. Our results have implications for both the understanding of bacterial social interactions within hosts, and therapeutic approaches that seek to take advantage of social dynamics between strains for infection control.

Numerous in-vitro studies have shown that cooperative bacterial cooperation can be exploited by cheating mutants that no longer express the social trait, but benefit from the cooperative acts performed by others (Griffin et al., 2004; Diggle et al., 2007; West et al., 2007; Ross-Gillespie et al., 2007; Sandoz et al., 2007; Kümmerli et al., 2009a, 2015; Popat et al., 2012; Ghoul et al., 2014; O'Brien et al., 2017; Özkaya et al., 2018). While these studies showed that cheating allows non-producers to out-compete producers, we found that the spread of non-producers was constraint within infections. There are multiple reasons that could explain this constraint. First, increased spatial structure is known to limit bacterial dispersal and the diffusion of secreted metabolites (Kümmerli et al., 2009a; Weigert and Kümmerli, 2017). As a consequence, metabolite sharing becomes more local, i.e. among clonal neighbors in growing microcolonies, which restricts non-producers in accessing the public goods. In infection systems such as ours, where bacteria attach to host tissue, spatial structure is likely high, and public good sharing might be limited. Indeed, as shown in Figure 6, co-infecting strains within the worm gut can be strongly spatially segregated, which could explain the limits of cheating. Taken together, our results are in line with work by Zhou *et al* (2014) who showed that QS-mutants of *Bacillus thuringiensis* infecting an insect caterpillar could

not exploit metabolites from producers because they were spatially separated in the host.

Second, negative frequency-dependent selection could explain why the spread of virulence factor negative mutants is constrained (Ross-Gillespie et al., 2007). This scenario predicts that cheaters only experience a selective advantage when rare, because then they are surrounded by producers and can exploit public goods most efficiently. At high frequency, meanwhile, non-producers might be selected against because the accessibility of public goods is reduced. The results from our competition assay provide indirect evidence for negative frequency-dependent selection in the nematode gut (Figure 5B). Specifically for mixed infections, we observed that bacterial load was reduced when producers occurred at low frequency early during infection (6 hpe), but not later on (48 hpe). This pattern is compatible with the view that rare producers have a selective advantage, increase in relative frequency and restore bacterial load.

Third, the relatively low bacterial density observed in the gut could further compromise the ability of non-producers to cheat (Figure 1D, 5B). Low cell density restricts the sharing and therefore also the exploitation of secreted compounds (Ross-Gillespie et al., 2009; Van Gestel et al., 2014; Scholz and Greenberg, 2015). Mechanisms that contribute to the persistent low bacterial density in the gut (Figure 1D, 5B) could include the peristaltic activity of the gut, constantly expelling a part of the pathogen population and the host

328 immune system, killing a fraction of the bacteria (Pukkila-Worley and Ausubel, 2012).

330

Fourth, our analysis reveals that the expression of pyoverdine and QS-
332 systems decline over time during host colonization (Figure 2). This could mean that the costs and benefits of shared virulence factors are reduced at later
334 stages of the infection, or that bacteria switch from the production to the recycling of already secreted public goods (Imperi et al., 2009; Kümmerli and
336 Brown, 2010). The spread of non-producers might be hampered in this case because the exploitability of a trait depends on its expression level (Kümmerli
338 et al., 2009b; Jiricny et al., 2010).

340 Finally, our analysis shows that the regulatory linkage between traits is an important factor to consider when predicting the putative advantage of non-
342 producers (Ross-Gillespie et al., 2015; Lindsay et al., 2016; dos Santos et al., 2018). For instance, we found that *P. aeruginosa* mutants deficient for
344 pyoverdine production upregulated pyochelin to compensate for the lack of their primary siderophore (Figure 3). Thus, if pyoverdine-negative mutants
346 evolve *de novo*, their spread as cheaters could be hampered because they invest in pyochelin as an alternative public good (Ross-Gillespie et al., 2015).
348 For QS, meanwhile, we observed that the absence of a functional Las-system resulted in the concomitant collapse of the Rhl-system. Although *lasR* mutants
350 could be potent cheats as they are deficient for multiple social traits, their spread might be hampered because QS-systems also regulate non-social
352 traits, which are important for individual fitness (Dandekar et al., 2012). In the

context of infections, *lasR*-mutants evolve frequently, with their spread being partly attributable to cheating, but also to modifications in the QS-hierarchy and a shift from a pathogenic to a commensalistic lifestyle (Jansen et al., 2015; Feltner et al., 2016; Granato et al., 2018).

When relating our work to previous studies, it turns out that earlier work produced mixed results with regard to the question whether siderophore- and QS-deficient mutants can spread in infections. Harrison *et al*. (2006, 2017; pyoverdine, *P. aeruginosa* in *Galleria mellonella* and a range of ex-vivo infection models) and Zhou *et al*. (2014; QS, *B. thuringiensis* in *Plutella xylostella*) showed that the spread of non-producers is constrained, whereas Rumbaugh *et al*. (2009, 2012; QS; *P. aeruginosa* in mice) and Pollitt *et al*. (2014; QS, *Staphylococcus aureus* in *G. mellonella*) demonstrated cases where non-producers spread to high frequencies in host populations. While the reported results were mainly based on count data (i.e. strain frequency before and after competition), we here show that information on social trait expression, temporal infection dynamics and physical interactions among strains within hosts are essential to understand whether social traits are important and exploitable in a given system (see also Zhou *et al*. (2014) for a similar approach regarding the spatial scale of strain interactions). Based on these novel insights, we posit that more of such detailed approaches are required to understand the importance of bacterial social interactions across host systems and infection contexts and explain differences between them.

A deeper understanding of bacterial social interactions inside hosts are particularly relevant for a number of novel therapeutic approaches that seek to take advantage of social dynamics between cooperative and cheating strains inside hosts to control infections. For instance, it was proposed that strains deficient for the production of important virulence factors could be introduced into established infections (Brown et al., 2009). These strains are expected to spread because of cheating, thereby reducing the overall virulence factor availability in the population, and consequently the damage to the host. Our results now reveal that cheater strains, although gaining a benefit from the presence of producer strains, are unable to spread in populations. Another therapeutic approach involves the specific targeting of secreted virulence factors to curb virulence (André and Godelle, 2005; Allen et al., 2014). This approach is thought to not only reduce damage to the host, but also to compromise resistance evolution (Pepper, 2012). The idea here is that resistant mutants, resuming virulence factor production, would act as cooperators, sharing the benefit of secreted goods with susceptible strains; and for this reason they are not expected to spread (Mellbye and Schuster, 2011; Gerdt and Blackwell, 2014; Ross-Gillespie et al., 2014). Our results now indicate that such cooperative drug-resistant mutants could get at least some local benefits and might increase to a certain frequency in the population (Rezzoagli et al., 2018). These confrontations show that the identification of key parameters driving social interactions across hosts and infection types is of utmost importance to predict the success of ‘cheat therapies’ and anti-virulence strategies targeting secreted public goods.

Material and methods

Strain and bacterial growth conditions

Bacterial strains, primers and plasmids used in this study are listed in Supplementary Tables S1-S3. Details on strain construction can be found in the Supplementary Methods. For all experiments, overnight cultures were grown in 8 ml Lysogeny broth (LB) medium in 50 ml Falcon tubes, incubated at 37°C, 220 rpm for 18 hours. We washed overnight cultures with 0.8% NaCl solution and adjusted them to OD_{600} = 1. Solid Nematode Growth Media (NGM) contained 0.25% Peptone, 50 mM NaCl, 25mM [PO_4^-], 5 µg/ml Cholesterol, 1mM $CaCl_2$, 1mM $MgSO_4$ supplemented with 1.5% agar. Agar plates (6 cm diameter) were seeded with 50 µl of bacterial culture and incubated at 25°C for 24 hours. All *P. aeruginosa* strains used in this study showed equal growth on NGM exposure plates (Supplementary Figure S4. Peptone was purchased from BD Biosciences, Switzerland, all other chemicals from Sigma Aldrich, Switzerland.

Nematode culture

We used the temperature-sensitive, reproductively sterile *C. elegans* strain JK509 (glp-1(q231) III): this strain is fertile at 16°C but does not develop gonads and is therefore sterile at 25°C. Worms were maintained at the permissive temperature (16°C) on High Growth Media (HGM) agar plates (2% Peptone, 50 mM NaCl, 25mM [PO_4^-], 20 µg/ml Cholesterol, 1mM $CaCl_2$, 1mM $MgSO_4$) seeded with the standard food source *E. coli* strain OP50 (Stiernagle, 2006). For age synchronization, plates were washed with sterile distilled water and worms were treated with hypochlorite-sodium hydroxide solution in order

to kill adults worm and isolate eggs (Stiernagle, 2006). These were placed in M9 buffer (20 mM KH_2PO_4, 40 mM Na_2HPO_4, 80 mM NaCl, 1 mM $MgSO_4$) and incubated at 16°C for 16-18 hours to hatch. Then, L1 larvae were transferred to HGM plates seeded with OP50 and incubated at 25°C for 28 hours to reach L4 developmental stage. Worms and the OP50 strain were provided by the Caenorhabditis Genetic Center (CGC), which is supported by the National Institutes of Health - Office of Research Infrastructure Programs (P40 OD010440).

C. elegans infection protocol

Synchronized L4 worms were washed off of HGM plates with M9 buffer + 50 µg/ml kanamycin (M9-Kan), and washed three times with M9-Kan for surface-disinfecting the worms. Bacteria, dead worms, and other debris or contamination were then separated from the viable worm population by the sucrose flotation method (Portman, 2006) and rinsed three time in M9 buffer to remove sucrose. The worm handling protocol for the main experiments is depicted in Figure 1A. Specifically, approximately 200 worms were moved to NGM plates containing a lawn of bacteria and incubated statically for 24 hours at 25°C. After this period of exposure to pathogens, infected worms were extensively washed with M9 buffer + 50 µg/ml chloramphenicol (M9-Cm) followed by M9 buffer, and subsequently transferred to individual wells of a 6-well culture plate filled with sterile M9 buffer supplemented with 5 µg/ml cholesterol (M9+Ch Buffer) where they were kept for a total of 48 hours post exposure (hpe) and imaged at timepoints 0, 6 and 30 hpe. This procedure allowed us to clearly distinguish between the initial uptake rate of bacteria

452 through feeding, and the subsequent colonization of the worm gut by surviving bacteria.

454

Nematode survival assay

456 Our primary goal was to observe infections inside living hosts and not to kill them. To verify that worms stayed alive during the experimental period (up to 458 time point 48 hpe), we tracked their survival by transferring a fraction of the infected population (50-90 worms) to individual wells filled with M9-Ch buffer. 460 Worms were observed for motility at 0, 24 and 48 hpe, by prodding them with a platinum wire. A worm was considered dead when it no longer responded to 462 touch. Each bacterial strain was tested in three replicates and three independent experiments were carried out. We used *E. coli* OP50 as a 464 negative control for killing. During this period of observation, the worms experienced only negligible killing by the colonizing bacteria, and we found no 466 significant difference in killing between the non-pathogenic *E. coli* food strain and the *P. aeruginosa* strains (Supplementary Figure S2). However, there was 468 a small but significant difference in the survival of worms colonized by the three siderophore-mutant strain, compared to the survival of worms infected 470 by the wildtype PAO1 (ANOVA with post-hoc Tukey test for multiple comparisons, $p = 0.0213$ for PAO1 Δ*pchEF*, $p = 0.0054$ for PAO1 Δ*pvdD* and 472 $p = 0.0062$ for PAO1 Δ*pvdD*Δ*pchEF*).

474 **Microscopy setup and imaging**

For observations under the microscope, we picked individual worms from the 476 M9+Ch buffer and paralyzed them with a 25 mM sodium azide solution before

transferring them to a 18-well µ-slide (Ibidi). Worms were observed at different time points: immediately after exposure (0 hpe), as well as after 6 and 30 hpe. All experiments were carried out at the Center for Microscope and Image Analysis of the University Zürich (ZMB). For the colonization experiment, images were acquired on a Leica LX inverted widefield light microscope system with the Leica TX2 filter cube for mCherry (emission: 560 ± 40 nm, excitation: 645 ± 75 nm, DM = 595) and a Leica DFC 350 FX, cooled fluorescence monochrome camera (resolution: 1392 × 1040 pixels) for image recording (16-bit color depth). For the gene expression experiment, microscopy was performed on the InCell Analyzer 2500HS (GE Healthcare) automated imaging system, using a polychroic beam splitter BGRFR_2 (for mCherry, excitation: 575 ± 25 nm, emission: 607.5 ± 19 nm) and a PCO – sCMOS camera (resolution: 2048 x 2048 pixels, 16-bit).

Image processing and analysis

To extract fluorescence measurements from individual worms, images were first segmented (i.e. we divided the image into objects and background), using an automated image segmentation workflow with the image analysis tool *ilastik* (Sommer et al., 2011). Segmented images were then imported in the free scientific image processing software package Fiji (Schindelin et al., 2012) and used to determine fluorescence intensity (as “Raw Integrated Density”, i.e. the sum of the values of the pixels in the selection) and area of each worm. Images obtained from the InCell microscope were acquired dividing each well of the slide in 64-frames (8x8 grid) with 10% overlap. Tiles were stitched together using a macro-automated version of the Stitching plugin in Fiji

(Preibisch et al., 2009) and then segmented and analyzed as described above. To correct for the autofluorescence of the background and the host tissue, we imaged, at each time point, worms infected with non-fluorescent strains such as *E.coli* OP50-I or PAO1 wildtype and used the mean intensity of these control infections to correct fluorescent values from worms infected with fluorescent strains.

Competition assay in the host

For in-vivo competitions between the wildtype PAO1-mCherry and the siderophore-negative strain PAO1 *ΔpvdDΔpchEF* or the lasR-mutant PAO1 *ΔlasR*, overnight monocultures were washed twice with 0.8% NaCl solution, adjusted to OD_{600} = 1 and mixed at 1:1 ratio. To control for fitness effects of the fluorescent marker mCherry, we also competed the untagged PAO1 wildtype against PAO1-mCherry. NGM plates were then seeded with 50 µl of mixed culture and incubated at 25°C for 24 hours. Worms were put on the mixed bacterial lawn for 24 hours and then recovered as previously described. After 6 and 48 hours post-exposure, individual worms were picked, immobilized with sodium azide and washed for 5 minutes with M9 + 0.003% NaOCl. Worms were washed twice with M9 buffer. We then transferred each individual worm to a 1.5 ml screw-cap micro tube (Sarstedt, Switzerland) containing sterilized glass beads (1 mm diameter, Sigma Aldrich). Worms were disrupted using a bead-beater (TissueLyser II, QIAGEN, Germany), shaking at 30 Hz for 1.5 min before flipping the tubes and shaking for an additional 1.5 min to ensure even disruption (adapted from Vega *et al.*, 2017). Tubes were then centrifuged at 2000 x g for 2 min, the content was re-

suspended in 200 µl of 0.8% NaCl and plated on two LB 1.2 % agar plates for each sample. Plates were incubated overnight at 37°C and left at room temperature for another 24 h to allow the fluorescent marker to fully mature. We then distinguished between fluorescent and non-fluorescent colonies using a custom built fluorescence imaging device (*Infinity 3* camera, Lumenera, Canada). We then calculated the relative fitness of the wildtype PAO1 as $\ln(v)=\ln\{[a_{48}\times(1-a_6)]/[a_6\times(1-a_{48})]\}$, where a_6 and a_{48} are the frequency of PAO1-mCherry at 6 and 48 hours after recovery, respectively (Ross-Gillespie et al., 2007). Values of $\ln(v)<0$ or $\ln(v)>0$ indicate whether the frequency of PAO1-mCherry increased ($\ln(v)< 0$) or decreased ($\ln(v)>0$) relative to its competitor.

Co-localization analysis

To determine the degree of co-localization of two different bacterial strains in the host, we transferred nematode worms to NGM plates seeded with a 1:1 ratio mix of PAO1-gfp with either PAO1-mCherry, PAO1 *ΔpvdDΔpchEF*–mCherry*,* or PAO1 *ΔlasR-mCherry*. After a grazing time of 24 hours, we picked single worms and imaged both the mCherry- and the GFP channel, using the InCell Analyzer 2500HS microscope as described above. For image analysis, we straightened each worm using the *Straighten* plugin in Fiji (Kocsis et al., 1991). We then used Fiji to extract fluorescence intensity values for each pixel in the worm from tail (X = 0) to head (X = 1), in both channels (green = GFP, red = mCherry). To ensure that we only measure areas where bacteria were present, we restricted our analysis to the region of the worm gut, where the colonization of the worm takes place. We then calculated the

552 Spearman correlation coefficient between the two fluorescent signals, as a proxy for co-localization of the two strains using the statistical software
554 RStudio (R Development Core Team, 2013).

556 **Statistical analysis**

All statistical analyses were performed in RStudio v. 3.3.0 (R Development
558 Core Team, 2013). We used Pearson correlations to test for associations between PAO1-mCherry fluorescence intensities and (a) recovered bacteria
560 from the gut; and (b) total bacterial load in mixed infections. We used analysis of variance (ANOVA) to compare fluorescence values between observation
562 times, strains and for comparisons to non-fluorescent controls. P-values were corrected for multiple comparisons using the post-hoc Tukey HSD test. To
564 compare promoter expression data between PAO1 WT and mutant strains, and to compare relative fitness values between competitors in the competition
566 assay, we used Welch's two-sample t-test. Co-localization analysis was performed using the Spearman correlation coefficient between the intensity
568 distribution of mCherry and GFP across the entire length of the worm. We tested for differences in co-localization between treatments using ANOVA.

570

Acknowledgments

572 We thank the Center of Microscopy and Image Analysis (University of Zürich) for support with image acquisition and advice on image analysis.

574

Funding

This work was funded by the Swiss National Science Foundation (grant no. PP00P3_165835 to RK), the European Research Council (grant no. 681295 to RK), and a Swiss National Science Foundation post-doctoral fellowship (no. P2ZHP3_174751 to EG).

Competing Interests

The authors have no competing interests to declare.

References:

Alibaud L, Köhler T, Coudray A, Prigent-Combaret C, Bergeret E, Perrin J, Benghezal M, Reimmann C, Gauthier Y, Van Delden C, Attree I, Fauvarque MO, Cosson P. 2008. Pseudomonas aeruginosa virulence genes identified in a Dictyostelium host model. *Cell Microbiol* **10**:729–740. doi:10.1111/j.1462-5822.2007.01080.x

Allen RC, Popat R, Diggle SP, Brown SP. 2014. Targeting virulence: can we make evolution-proof drugs? *Nat Rev Microbiol* **12**:300–308. doi:10.1038/nrmicro3232

Andersen SB, Ghoul M, Marvig RL, Lee Z-B, Molin S, Johansen HK, Griffin AS. 2018. Privatisation rescues function following loss of cooperation. *bioRxiv*. doi:10.1101/326165

Andersen SB, Marvig RL, Molin S, Krogh Johansen H, Griffin AS. 2015. Long-term social dynamics drive loss of function in pathogenic bacteria. *Proc Natl Acad Sci* **112**:10756–10761. doi:10.1073/pnas.1508324112

André JB, Godelle B. 2005. Multicellular organization in bacteria as a target for drug therapy. *Ecol Lett* **8**:800–810. doi:10.1111/j.1461-0248.2005.00783.x

Balasubramanian D, Schneper L, Kumari H, Mathee K. 2013. A dynamic and intricate regulatory network determines Pseudomonas aeruginosa virulence. *Nucleic Acids Res* **41**:1–20. doi:10.1093/nar/gks1039

Bao Y, Lies DP, Fu H, Roberts GP. 1991. An improved Tn7-based system for the single-copy insertion of cloned genes into chromosomes of gram-

606 negative bacteria. *Gene* **109**:167–168. doi:https://doi.org/10.1016/0378-1119(91)90604-A

608 Becker KW, Skaar EP. 2014. Metal limitation and toxicity at the interface between host and pathogen. *FEMS Microbiol Rev*. doi:10.1111/1574-6976.12087

610

Brown SP, West S a, Diggle SP, Griffin AS. 2009. Social evolution in micro-organisms and a Trojan horse approach to medical intervention strategies. *Philos Trans R Soc Lond B Biol Sci* **364**:3157–3168. doi:10.1098/rstb.2009.0055

612

614

Buckling A, Brockhurst MA. 2008. Kin selection and the evolution of virulence. *Heredity (Edinb)* **100**:484–488. doi:10.1038/sj.hdy.6801093

616

Cezairliyan B, Vinayavekhin N, Grenfell-Lee D, Yuen GJ, Saghatelian A, Ausubel FM. 2013. Identification of Pseudomonas aeruginosa phenazines that kill Caenorhabditis elegans. *PLoS Pathog* **9**:e1003101. doi:10.1371/journal.ppat.1003101

618

620

Choi K-H, Schweizer HP. 2006. mini-Tn7 insertion in bacteria with single attTn7 sites: example Pseudomonas aeruginosa. *Nat Protoc* **1**:153–161. doi:10.1038/nprot.2006.24

622

624 Clatworthy AE, Pierson E, Hung DT. 2007. Targeting virulence: a new paradigm for antimicrobial therapy. *Nat Chem Biol* **3**:541–548. doi:10.1038/nchembio.2007.24

626

Cornelis P, Dingemans J. 2013. *Pseudomonas aeruginosa* adapts its iron uptake strategies in function of the type of infections. *Front Cell Infect Microbiol* **3**:1–7. doi:10.3389/fcimb.2013.00075

628

630 Dandekar AA, Chugani S, Greenberg PE. 2012. Bacterial Quorum Sensing and Metabolic Incentives to Cooperate. *Science (80-)* **338**:264–266. doi:110.1126/science.1227289.

632

Diggle SP, Griffin AS, Campbell GS, West S a. 2007. Cooperation and conflict in quorum-sensing bacterial populations. *Nature* **450**:411–414. doi:10.1038/nature06279

634

636 dos Santos M, Ghoul M, West SA. 2018. Pleiotropy, cooperation and the social evolution of genetic architecture. *PLoS Biol* **16**:e2006671. doi:10.1371/journal.pbio.2006671

638

Dumas Z, Ross-Gillespie A, Kümmerli R. 2013. Switching between apparently redundant iron-uptake mechanisms benefits bacteria in changeable environments. *Proc Biol Sci* **280**:20131055. doi:10.1098/rspb.2013.1055

Ewbank JJ. 2002. Tackling both sides of the host – pathogen equation with Caenorhabditis elegans **4**:247–256. doi:10.1016/S1286-4579(01)01531-3

Félix M-A, Braendle C. 2010. The natural history of Caenorhabditis elegans. *Curr Biol* **20**:R965–R969. doi:10.1016/J.CUB.2010.09.050

Feltner JB, Wolter DJ, Pope CE, Groleau M, Smalley NE, Greenberg EP. 2016. LasR Variant Cystic Fibrosis Isolates Reveal an Adaptable Quorum- Sensing Hierarchy in Pseudomonas aeruginosa. *MBio* **7**:e01513-16. doi:10.1128/mBio.01513-16.

Flemming HC, Wingender J, Szewzyk U, Steinberg P, Rice SA, Kjelleberg S. 2016. Biofilms: An emergent form of bacterial life. *Nat Rev Microbiol* **14**:563–575. doi:10.1038/nrmicro.2016.94

Gerdt JP, Blackwell HE. 2014. Competition Studies Confirm Two Major Barriers That Can Preclude the Spread of Resistance to Quorum-Sensing Inhibitors in Bacteria. *ACS Chem Biol* **9**:2291–2299. doi:10.1021/cb5004288

Ghoul M, Griffin AS, West SA. 2014. Toward an evolutionary definition of cheating. *Evolution (N Y)* **68**:318–331. doi:10.1111/evo.12266

Granato ET, Harrison F, Kümmerli R, Ross-Gillespie A. 2016. Do Bacterial "Virulence Factors" Always Increase Virulence? A Meta-Analysis of Pyoverdine Production in Pseudomonas aeruginosa As a Test Case. *Front Microbiol* **7**:1952. doi:10.3389/fmicb.2016.01952

Granato ET, Ziegenhain C, Marvig RL, Kümmerli R. 2018. Low spatial structure and selection against secreted virulence factors attenuates pathogenicity in Pseudomonas aeruginosa. *ISME J*. doi:10.1038/s41396-018-0231-9

Griffin AS, West SA, Buckling A. 2004. Cooperation and competition in pathogenic bacteria. *Nature* **430**:1024–1027. doi:10.1038/nature02744

Harrison F. 2013. Bacterial cooperation in the wild and in the clinic: Are pathogen social behaviours relevant outside the laboratory? *BioEssays* **35**:108–112. doi:10.1002/bies.201200154

672 Harrison F, Browning LE, Vos M, Buckling A. 2006. Cooperation and virulence in acute Pseudomonas aeruginosa infections. *BMC Biol*.
674 doi:10.1186/1741-7007-4-21

Harrison F, McNally A, Da Silva AC, Heeb S, Diggle SP. 2017. Optimised
676 chronic infection models demonstrate that siderophore “cheating” in Pseudomonas aeruginosa is context specific. *ISME J* **11**:2492–2509.
678 doi:10.1038/ismej.2017.103

Henkel JS, Baldwin MR, Barbieri JT. 2010. Toxins from bacteria. *EXS* **100**:1–
680 29. doi:10.1007/978-3-7643-8338-1_1

Imperi F, Tiburzi F, Visca P. 2009. Molecular basis of pyoverdine siderophore
682 recycling in Pseudomonas aeruginosa. *Proc Natl Acad Sci* **106**:20440–20445. doi:10.1073/pnas.0908760106

684 Jansen G, Crummenerl LL, Gilbert F, Mohr T, Pfefferkorn R, Thänert R, Rosenstiel P, Schulenburg H. 2015. Evolutionary Transition From
686 Pathogenicity To Commensalism: Global Regulator Mutations Mediate Fitness Gains Through Virulence Attenuation. *Mol Biol Evol* **32**:2883–
688 2896. doi:10.1093/molbev/msv160

Jiricny N, Diggle SP, West SA, Evans BA, Ballantyne G, Ross-Gillespie A,
690 Griffin AS. 2010. Fitness correlates with the extent of cheating in a bacterium. *J Evol Biol* **23**:738–747. doi:10.1111/j.1420-
692 9101.2010.01939.x

Kirienko N V., Kirienko DR, Larkins-Ford J, W??hlby C, Ruvkun G, Ausubel
694 FM. 2013. Pseudomonas aeruginosa disrupts Caenorhabditis elegans iron homeostasis, causing a hypoxic response and death. *Cell Host*
696 *Microbe* **13**:406–416. doi:10.1016/j.chom.2013.03.003

Kocsis E, Trus BL, Steer CJ, Bisher ME, Steven AC. 1991. Image averaging of
698 flexible fibrous macromolecules: the clathrin triskelion has an elastic proximal segment. *J Struct Biol* **107**:6–14. doi:10.1016/1047-
700 8477(91)90025-R

Köhler T, Buckling A, van Delden C. 2009. Cooperation and virulence of
702 clinical Pseudomonas aeruginosa populations. *Proc Natl Acad Sci* **106**:6339–6344. doi:10.1073/pnas.0811741106

704 Kümmerli R, Brown SP. 2010. Molecular and regulatory properties of a public

good shape the evolution of cooperation. *Proc Natl Acad Sci U S A* **107**:18921–6. doi:10.1073/pnas.1011154107

Kümmerli R, Griffin AS, West S a, Buckling A, Harrison F. 2009a. Viscous medium promotes cooperation in the pathogenic bacterium *Pseudomonas aeruginosa*. *Proc Biol Sci* **276**:3531–3538. doi:10.1098/rspb.2009.0861

Kümmerli R, Jiricny N, Clarke LS, West SA, Griffin AS. 2009b. Phenotypic plasticity of a cooperative behaviour in bacteria. *J Evol Biol* **22**:589–598. doi:10.1111/j.1420-9101.2008.01666.x

Kümmerli R, Santorelli LA, Granato ET, Dumas Z, Dobay A, Griffin AS, West SA. 2015. Co-evolutionary dynamics between public good producers and cheats in the bacterium Pseudomonas aeruginosa. *J Evol Biol* **28**:2264–74. doi:10.1111/jeb.12751

Lee J, Zhang L. 2015. The hierarchy quorum sensing network in Pseudomonas aeruginosa. *Protein Cell* **6**:26–41. doi:10.1007/s13238-014-0100-x

Leggett HC, Brown SP, Reece SE. 2014. War and peace□: social interactions in infections. *Philos Trans R Soc B* **369**:20130365. doi:http://dx.doi.org/10.1098/rstb.2013.0365

Lindsay RJ, Kershaw MJ, Pawlowska BJ, Talbot NJ, Gudelj I. 2016. Harbouring public good mutants within a pathogen population can increase both fitness and virulence. *Elife* **5**:1–25. doi:10.7554/eLife.18678

Mahajan-Miklos S, Tan MW, Rahme LG, Ausubel FM. 1999. Molecular mechanisms of bacterial virulence elucidated using a Pseudomonas aeruginosa-Caenorhabditis elegans pathogenesis model. *Cell* **96**:47–56. doi:10.1016/S0092-8674(00)80958-7

Mellbye B, Schuster M. 2011. The sociomicrobiology of antivirulence drug resistance: a proof of concept. *MBio* **2**:e00131-11. doi:10.1128/mBio.00131-11

Meyer JM, Neely A, Stintzi A, Georges C, Holder IA. 1996. Pyoverdin is essential for virulence of Pseudomonas aeruginosa. *Infect Immun* **64**:518–523.

Nadal Jimenez P, Koch G, Thompson J a., Xavier KB, Cool RH, Quax WJ. 2012. The Multiple Signaling Systems Regulating Virulence in

738 Pseudomonas aeruginosa. *Microbiol Mol Biol Rev* **76**:46–65. doi:10.1128/MMBR.05007-11

740 O'Brien S, Luján AM, Paterson S, Cant MA, Buckling A. 2017. Adaptation to public goods cheats in Pseudomonas aeruginosa. *Proc R Soc B Biol Sci* 742 **284**:20171089. doi:10.1098/rspb.2017.1089

Özkaya Ö, Balbontín R, Gordo I, Xavier KB. 2018. Cheating on Cheaters 744 Stabilizes Cooperation in Pseudomonas aeruginosa. *Curr Biol* **26**:2070–2080. doi:10.1016/j.cub.2018.04.093

746 Papaioannou E, Utari P, Quax W. 2013. Choosing an Appropriate Infection Model to Study Quorum Sensing Inhibition in Pseudomonas Infections. *Int* 748 *J Mol Sci* **14**:19309–19340. doi:10.3390/ijms140919309

Papaioannou E, Wahjudi M, Nadal-Jimenez P, Koch G, Setroikromo R, Quax 750 WJ. 2009. Quorum-quenching acylase reduces the virulence of Pseudomonas aeruginosa in a Caenorhabditis elegans infection model. 752 *Antimicrob Agents Chemother*. doi:10.1128/AAC.00380-09

Parrow NL, Fleming RE, Minnick MF. 2013. Sequestration and scavenging of 754 iron in infection. *Infect Immun*. doi:10.1128/IAI.00602-13

Pepper JW. 2012. Drugs that target pathogen public goods are robust against 756 evolved drug resistance. *Evol Appl* **5**:757–761. doi:10.1111/j.1752-4571.2012.00254.x

758 Pollitt EJG, West SA, Crusz SA, Burton-Chellew MN, Diggle SP. 2014. Cooperation, quorum sensing, and evolution of virulence in 760 Staphylococcus aureus. *Infect Immun* **82**:1045–1051. doi:10.1128/IAI.01216-13

762 Popat R, Crusz S a., Messina M, Williams P, West S a., Diggle SP. 2012. Quorum-sensing and cheating in bacterial biofilms. *Proc R Soc B Biol Sci* 764 **279**:4765–4771. doi:10.1098/rspb.2012.1976

Portal-Celhay C, Bradley ER, Blaser MJ. 2012. Control of intestinal bacterial 766 proliferation in regulation of lifespan in Caenorhabditis elegans. *BMC Microbiol* **12**:49. doi:10.1186/1471-2180-12-49

768 Portman DS. 2006. Profiling C. elegans gene expression with DNA microarrays In: Community TC elegan. R, editor. WormBook: The Online 770 Review of C. Elegans Biology. WormBook.

Preibisch S, Saalfeld S, Tomancak P. 2009. Globally optimal stitching of tiled 3D microscopic image acquisitions. *Bioinformatics* **25**:1463–1465. doi:10.1093/bioinformatics/btp184

Priefer UB, Simon R, Pühler A. 1985. Extension of the Host Range of Escherichia coli Vectors by Incorporation of RSF1010 Replication and Mobilization Functions. *J Bacteriol* 324–330.

Pukkila-Worley R, Ausubel FM. 2012. Immune defense mechanisms in the Caenorhabditis elegans intestinal epithelium. *Curr Opin Immunol* **24**:3–9. doi:10.1016/j.coi.2011.10.004

R Development Core Team. 2013. R: A language and environment for statistical computing.R Foundation for Statistical Computing. Vienna, Austria.

Rahme LG, Stevens EJ, Wolfort SF, Shao J, Tompkins RG, Ausubel FM. 1995. Common virulence factors for bacterial pathogenicity in plants and animals. *Science (80-)* **268**:1899–902. doi:10.1126/science.7604262

Rasko DA, Sperandio V. 2010. Anti-virulence strategies to combat bacteria-mediated disease. *Nat Rev Drug Discov* **9**:117–128. doi:10.1038/nrd3013

Raymond B, West SA, Griffin AS, Bonsall MB. 2012. The dynamics of cooperative bacterial virulence in the field. *Science (80-)* **337**:85–88. doi:10.1126/science.1218196

Rezzoagli C, Wilson D, Weigert M, Wyder S, Kümmerli R. 2018. Probing the evolutionary robustness of two repurposed drugs targeting iron uptake in Pseudomonas aeruginosa. *Evol Med Public Heal* **1**:246–259. doi:10.1093/emph/eoy026

Ross-Gillespie A, Dumas Z, Kümmerli R. 2015. Evolutionary dynamics of interlinked public goods traits: An experimental study of siderophore production in Pseudomonas aeruginosa. *J Evol Biol* **28**:29–39. doi:10.1111/jeb.12559

Ross-Gillespie A, Gardner A, Buckling A, West SA, Griffin AS. 2009. Density dependence and cooperation: theory and a test with bacteria. *Evolution* **63**:2315–2325. doi:10.1111/j.1558-5646.2009.00723.x

Ross-Gillespie A, Gardner A, West SA, Griffin AS. 2007. Frequency dependence and cooperation: theory and a test with bacteria. *Am Nat*

170:331–342. doi:10.1086/519860

Ross-Gillespie A, Weigert M, Brown SP, Kümmerli R. 2014. Gallium-mediated siderophore quenching as an evolutionarily robust antibacterial treatment. *Evol Med Public Heal* **2014**:18–29. doi:10.1093/emph/eou003

Rumbaugh KP, Diggle SP, Watters CM, Ross-Gillespie A, Griffin AS, West SA. 2009. Quorum Sensing and the Social Evolution of Bacterial Virulence. *Curr Biol* **19**:341–345. doi:10.1016/J.CUB.2009.01.050

Rumbaugh KP, Trivedi U, Watters C, Burton-Chellew MN, Diggle SP, West SA. 2012. Kin selection, quorum sensing and virulence in pathogenic bacteria. *Proc R Soc B Biol Sci* **279**:3584–3588. doi:10.1098/rspb.2012.0843

Sandoz KM, Mitzimberg SM, Schuster M. 2007. Social cheating in Pseudomonas aeruginosa quorum sensing. *Proc Natl Acad Sci U S A* **104**:15876–81. doi:10.1073/pnas.0705653104

Schindelin J, Arganda-Carreras I, Frise E, Kaynig V, Longair M, Pietzsch T, Preibisch S, Rueden C, Saalfeld S, Schmid B, Tinevez J-Y, White DJ, Hartenstein V, Eliceiri K, Tomancak P, Cardona A. 2012. Fiji: an open-source platform for biological-image analysis. *Nat Methods* **9**:676–82. doi:10.1038/nmeth.2019

Scholz RL, Greenberg EP. 2015. Sociality in Escherichia coli: Enterochelin Is a Private Good at Low Cell Density and Can Be Shared at High Cell Density. *J Bacteriol* **197**:2122–2128. doi:10.1128/JB.02596-14.

Smith RS, Iglewski BH. 2003. *P. aeruginosa* quorum-sensing systems and virulence. *Curr Opin Microbiol* **6**:56–60. doi:10.1016/S1369-5274(03)00008-0

Sommer C, Strähle C, Köthe U, Hamprecht FA. 2011. ilastik: Interactive Learning and Segmentation Toolkit.Eighth IEEE International Symposium on Biomedical Imaging (ISBI). Proceedings. pp. 230–233.

Stiernagle T. 2006. Maintenance of C. elegans. In: The C.elegans Research Community, editor. WormBook: The Online Review of C. Elegans Biology.

Takase H, Nitanai H, Hoshino K, Otani T. 2000. Impact of Siderophore Production on Pseudomonas aeruginosa Infections in Immunosuppressed Mice. *Infect Immun* **68**:1834–1839. doi:10.1128/IAI.68.4.1834-1839.2000

Tan MW, Ausubel FM. 2000. Caenorhabditis elegans: A model genetic host to study Pseudomonas aeruginosa pathogenesis. *Curr Opin Microbiol* **3**:29–34. doi:10.1016/S1369-5274(99)00047-8

Tan MW, Mahajan-Miklos S, Ausubel FM. 1999. Killing of Caenorhabditis elegans by Pseudomonas aeruginosa used to model mammalian bacterial pathogenesis. *Proc Natl Acad Sci U S A* **96**:715–20. doi:10.1073/pnas.96.2.715

Utari PD, Quax WJ. 2013. Caenorhabditis elegans reveals novel Pseudomonas aeruginosa virulence mechanism. *Trends Microbiol* **21**:315–316. doi:10.1016/j.tim.2013.04.006

Van Gestel J, Weissing FJ, Kuipers OP, Kovács ÁT. 2014. Density of founder cells affects spatial pattern formation and cooperation in Bacillus subtilis biofilms. *ISME J* **8**:2069–2079. doi:10.1038/ismej.2014.52

Vega NM, Gore J, Janczyk M, Dale R, Freeman J, Casadei G. 2017. Stochastic assembly produces heterogeneous communities in the Caenorhabditis elegans intestine. *PLOS Biol* **15**:e2000633. doi:10.1371/journal.pbio.2000633

Weigert M, Kümmerli R. 2017. The physical boundaries of public goods cooperation between surface-attached bacterial cells. *Proc R Soc B Biol Sci* **284**:20170631. doi:10.1098/rspb.2017.0631

West SA, Buckling A. 2003. Cooperation, virulence and siderophore production in bacterial parasites. *Proc R Soc Lond B* **270**:37–44. doi:10.1098/rspb.2002.2209

West SA, Diggle SP, Buckling A, Gardner A, Griffin AS. 2007. The Social Lives of Microbes. *Annu Rev Ecol Evol Syst* **38**:53–77. doi:10.1146/annurev.ecolsys.38.091206.095740

Wu HJ, Wang AHJ, Jennings MP. 2008. Discovery of virulence factors of pathogenic bacteria. *Curr Opin Chem Biol* **12**:93–101. doi:10.1016/j.cbpa.2008.01.023

Zaborin A, Romanowski K, Gerdes S, Holbrook C, Lepine F, Long J, Poroyko V, Diggle SP, Wilke A, Righetti K, Morozova I, Babrowski T, Liu DC, Zaborina O, Alverdy JC. 2009. Red death in Caenorhabditis elegans caused by Pseudomonas aeruginosa PAO1. *Proc Natl Acad Sci*

106:6327–32. doi:10.1073/pnas.0813199106

Zhou L, Slamti L, Nielsen-LeRoux C, Lereclus D, Raymond B. 2014. The Social Biology of Quorum Sensing in a Naturalistic Host Pathogen System. *Curr Biol* **24**:2417–2422. doi:10.1016/J.CUB.2014.08.049

Zhu J, Cai X, Harris TL, Gooyit M, Wood M, Lardy M, Janda KD. 2015. Disarming pseudomonas aeruginosa virulence factor lasb by leveraging a caenorhabditis elegans infection model. *Chem Biol* **22**:483–491. doi:10.1016/j.chembiol.2015.03.012

Figure captions

Figure 1. Quantifying *P. aeruginosa* infections in the *C. elegans* gut. (A) Experimental procedure: we used fluorescently tagged *P. aeruginosa* strains to examine bacterial colonization of the *C. elegans* gut. Per experiment, we exposed approximately 200 *C. elegans* nematodes to a lawn of mCherry-tagged PAO1 strains for 24 hours. Subsequently, nematodes were removed from the bacterial plate, surface washed and collected in sterile buffer for monitoring. After 0, 6, or 30 hours post exposure (hpe), approximately 30 nematodes were immobilized and transferred to microscopy slides for imaging. (B) Brightfield and fluorescence channel merged image depicting mCherry-fluorescent bacteria inside the host gut. (C) Bacterial load inside the nematode was quantified as the sum of fluorescence intensity across pixels in the region of interest "ROI" (yellow outline) and standardised by total worm area. (D) Colonization dynamics of the wildtype strain PAO1-mCherry: immediately after removal from the exposure plate (0 hpe), worms showed high bacterial loads inside their guts. Bacterial load first declined when the worms where kept in buffer for 6 hours, but then remained constant for the next 24 hours. Grey shaded area indicates background fluorescence (mean +/- standard deviation) of worms exposed to the non-fluorescent, non-pathogenic *E.coli* OP50. N = number of worms from four independent experiments. *** = $p < 0.001$, n.s. = not statistically significant.

Figure 2. *P. aeruginosa* expresses genes for pyoverdine synthesis and quorum sensing regulators in the host gut. To quantify the expression of virulence factor genes inside hosts, worms were exposed to four PAO1 strains, each containing a promoter::mCherry fusion for either *pvdA* (pyoverdine synthesis), *pchEF* (pyochelin synthesis), *lasR* or *rhlR* (quorum sensing regulators). With the exception of *pchEF*, all genes were significantly expressed in the host, both at 0 and 30 hpe. Expression levels were standardised for bacterial load. Grey shaded areas depict background fluorescence (mean +/- standard deviation) of worms exposed to the non-fluorescent, non-pathogenic *E.coli* OP50. N = number of worms from four

independent experiments. * = p < 0.05; ** = p < 0.01, *** = p < 0.001, n.s. = not
912 statistically significant.

914 **Figure 3. *P. aeruginosa* can switch between siderophores, while quorum sensing regulators act hierarchically.** Because virulence traits are linked at
916 the regulatory level, we measured gene expression of each trait in the negative background of the co-regulated trait. (A) The expression of the
918 pyoverdine synthetic gene *pvdA* is significantly expressed in the wildtype and the pyochelin-negative background, but slightly reduced in the latter. (B) The
920 pyochelin synthetic gene *pchEF* is significantly expressed in the pyoverdine-negative background, but silent in the wildtype. (C) The expression of the QS-
922 regulator gene *lasR* is unchanged in the Rhl-negative background compared to the wildtype. (D) The expression of the QS-regulator gene *rhlR* is reduced in
924 the Las-negative background. Expression levels were standardised for bacterial load. Grey shaded areas depict background fluorescence (mean +/-
926 standard deviation) of worms exposed to the non-fluorescent, non-pathogenic *E.coli* OP50. N = number of worms form four independent experiments. * = p <
928 0.05; ** = p < 0.01, *** = p < 0.001, n.s. = not statistically significant.

930 **Figure 4. Virulence factor production affects bacterial uptake and host colonization ability** (A) Bacterial load inside *C. elegans* guts measured
932 immediately after the recovery of worms from the exposure plates (0 hours post exposure; hpe). Comparisons across isogenic PAO1 mutant strains, each
934 deficient for the production of one or two virulence factors, reveal that the two quorum-sensing mutants PAO1 Δ*lasR* and PAO1 Δ*rhlR* reached lower
936 bacterial densities than the wildtype. (B) Comparison of the relative colonization success of strains (ratio of bacterial loads at 0 hpe versus 30 hpe)
938 revealed that the siderophore-negative strain PAO1 *ΔpvdDΔpchEF* showed significantly reduced ability to remain in the host compared to the wildtype. In
940 contrast, the colonisation success of PAO1 Δ*pchEF* and PAO1 Δ*rhlR* was increased relative to the wildtype. Grey shaded areas depict background
942 fluorescence (mean +/- standard deviation) of worms exposed to the non-fluorescent, non-pathogenic *E.coli* OP50. N = number of worms form four

944 independent experiments. * = $p < 0.05$; ** = $p < 0.01$, *** = $p < 0.001$.

946 **Figure 5. Mixed infections reveal social strain dynamics but no successful cheating** (A) Relative fitness of the wildtype PAO1-mCherry after
948 42 hours of competition inside the *C. elegans* gut against an untagged PAO1 control strain (white circles); the siderophore-negative strain PAO1
950 Δ*pvdD*Δ*pchEF* (green diamonds); and the Las-negative strain PAO1 Δ*lasR* (blue squares). The control competition revealed a mild but significant
952 negative effect of the mCherry tag on wildtype fitness. When accounting for these mCherry costs, we found that the putative cheat strains PAO1 Δ*lasR*
954 and PAO1 Δ*pvdD*Δ*pchEF* performed equally well compared to the wildtype, but could not outcompete it. This suggests that virulence factor deficient
956 strains benefit from the presence of non-producers but cannot successfully cheat on them. (B) At 6 hpe, wildtype frequency in mixed infections correlated
958 positively with total bacterial load inside hosts in competition with PAO1 Δ*lasR* (blue line) and PAO1 Δ*pvdD*Δ*pchEF* (green line) but not in the control
960 competition (grey line). (C) These correlations disappeared at 48 hpe. Each data point represents an individual worm. Data stems from three independent
962 experiments, with 8 replicates each.

964 **Figure 6. Spatial structure of mixed infections in the nematode gut.** (A, B) Illustrative examples of *C. elegans* individuals infected with a mixture of GFP-
966 and mCherry-labelled strains. Each worm was computationally straightened and fluorescence intensity values were extracted for each pixel from tail (X=0)
968 to head (X=1). We then calculated the Spearman correlation coefficient between the intensity values in the two fluorescence channels across pixels,
970 as our estimate of strain colocalization. Examples show worms with high (A) and low (B) degrees of colocalization. (C) Patterns of colocalization levels
972 varied substantially between individuals, but did not differ across strain combinations ($p = 0.119$: wildtype PAO1-mCherry versus: (i) wildtype PAO1-
974 gfp (white circles), (ii) PAO1 Δ*pvdD*Δ*pchEF*-mCherry (green diamonds) or (iii) PAO1 Δ*lasR*-mCherry (blue squares). Each data point represents an individual
976 worm. Data stems from 3 independent experiments, with 12 replicates each.

Supplementary Figures captions

Supplementary Figure S1. Fluorescence intensity significantly correlates with live bacteria inside the host gut. To assess the relationship between fluorescence signal and bacterial load inside *C. elegans*, colonized nematodes were observed using fluorescence microscopy and disrupted to extract live bacteria from the gut. Fluorescence intensity significantly correlated with the number of bacteria present in the host gut. (A) The correlation was moderate when the worms were observed immediately after exposure (0 hours post exposure; hpe) (Pearson correlation coefficient r = 0.496; test for association between paired samples t_{28} = 3.02, p = 0.0053). (B) At 6 hpe, fluorescence intensity correlated more strongly with bacterial load in the host gut (Pearson correlation coefficient r = 0.713; test for association between paired samples t_{23} = 4.88, p < 0.0001). In total, 65 worms were observed in two independent experiments. Fluorescence intensity values were blank corrected, using worms infected with the untagged strain PAO1 as non-fluorescent controls.

Supplementary Figure S2. Survival assay of worms infected with various *P. aeruginosa* strains. After washing worms off the exposure plates, we estimated host survival over 48 hours. For this purpose, we observed 50 to 90 worms and checked for viability every 24 hours by prodding them with a platinum wire three times. Worms were considered dead if they no longer moved upon stimulation with the wire . We found no significant difference in the survival rate between any of the strains compared to the food strain *E.coli* OP50-I (linear model, $F_{6,210}$ = 0.60, p = 0.7296). However, we found a small but significant difference in the survival of worms colonized by the three siderophore-mutants, which was higher compared to the survival of worms exposed to PAO1 (Tukey's range test, p = 0.0213 for PAO1 Δ*pchEF*, p = 0.0054 for PAO1 Δ*pvdD* and p = 0.0062 for PAO1 Δ*pvdD*Δ*pchEF*). Data points depict average survival across three independent experiments. In each experiment, we had three replicates for each strain. Gray areas represent the standard error of the mean.

Supplementary Figure S3. Bacterial load declines at 6 hours post exposure (hpe). We kept infected nematodes in sterile buffer and determined the fluorescence intensity in the host gut, reflecting the number of bacteria that managed to colonize the worms at 6 hpe. When scaled to the bacterial load at 0 hpe, we found that all strains showed a significant reduction in bacterial load. Moreover, the siderophore-negative strain PAO1 Δ *pvdD* Δ *pchEF* showed significantly reduced ability to remain in the host compared to PAO1 (ANOVA with post-hoc Tukey test, $t_{888} = -2.25$, $p = 0.0025$). For each individual strain, relative fluorescence is expressed as fluorescence intensity at 6 hpe scaled for the intensity at 0 hpe.

Supplementary Figure S4. Growth of *P. aeruginosa* WT and mutant strains for social traits on NGM plates. To assess the growth ability of PAO1 and the mutant strains on NGM plates, after 24 hours of incubation at 25°C, we collected the bacterial lawn in sterile NaCl solution and the OD600 was measured as proxy for cell growth. We found no statistically significant difference between strains (linear model $F_{5,60} = 2.27$, $p = 0.0588$). Data is shown as mean across four independent experiments, with three replicates (i.e. plates) per strain for each experiment. Error bars denote the standard error of the mean.

Supplementary Figure S5. Interaction between social traits inside the host at 30 hours post exposure. We compared the expression of promoter fusions inserted either in the wildtype PAO1 or in mutant strains, which lack either the second siderophore (light grey boxplot) or the second QS-regulator (white bars), at 30 hpe. Although values are generally lower, we observed the same trend as in Figure 3. Values are corrected for cell density. N = number of worms tested. Error bars represent standard errors of the mean. Grey shaded areas indicate the non-fluorescent background (mean +/- standard deviation). *** = $p < 0.001$ and n.s. = not statistically significant, based on Welch's 2-sample t-test between PAO1 and the respective mutant strain.

A

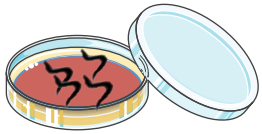

Nematodes washed with buffer + antibiotic

0 hpe

6 hpe

30 hpe

Nematodes immobilized (25 mM NaN_3)

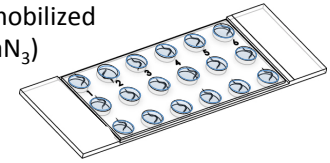

Exposure

Host exposed to mCherry-tagged *P. aeruginosa* strains for 24 h

Observation and measurements

Removal from exposure plate, collection in sterile buffer and microscopy measurement taken at 0, 6 and 30 hours post exposure (hpe).

B

C

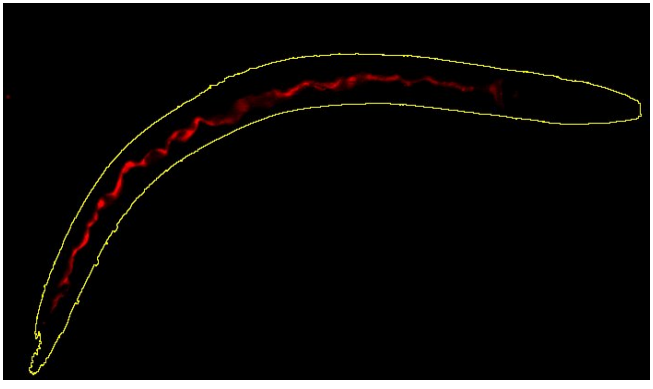

D

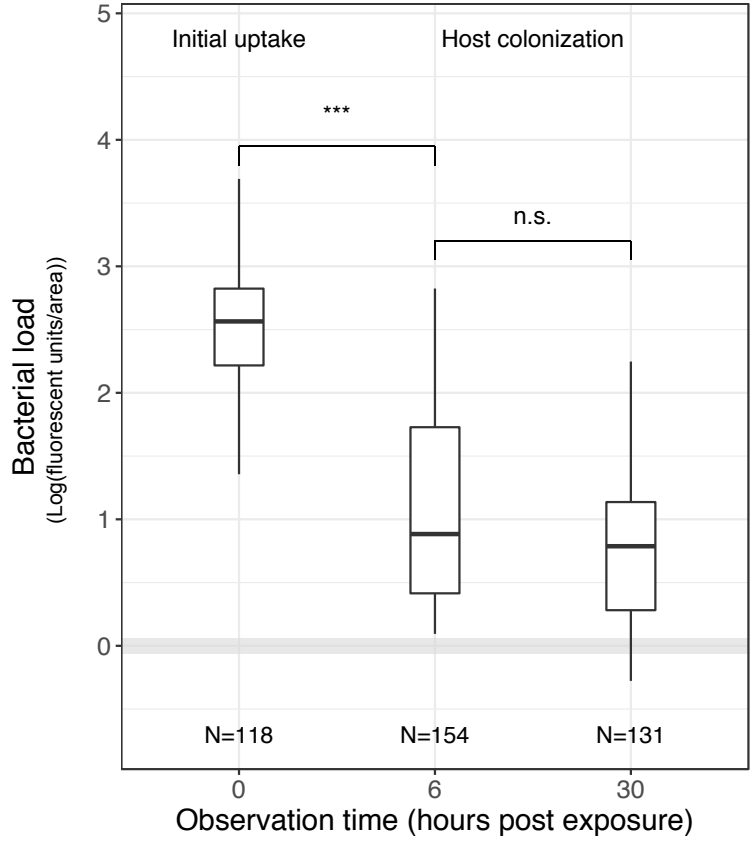

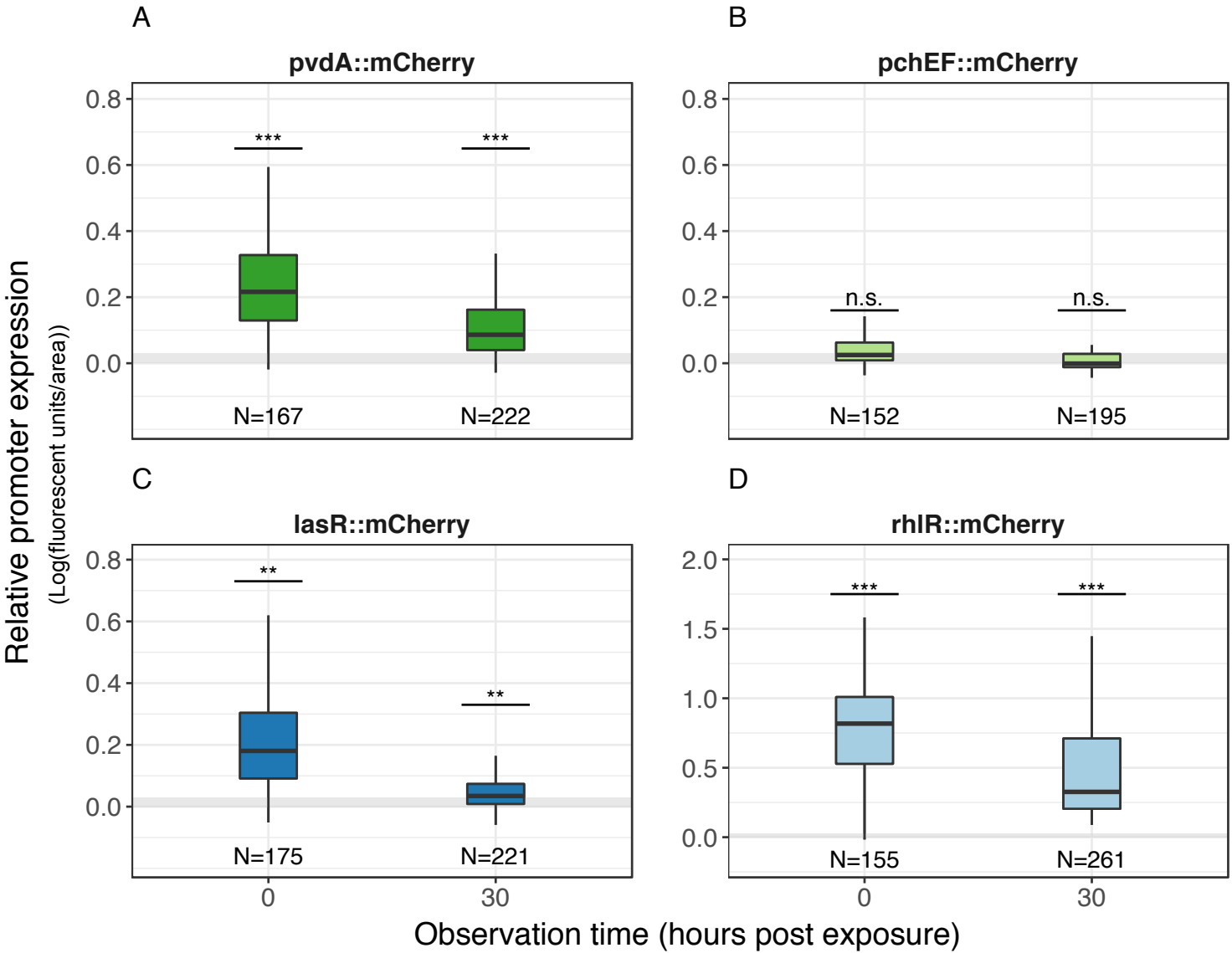
A
pvdA::mCherry
B
pchEF::mCherry
C
lasR::mCherry
D
rhlR::mCherry
Relative promoter expression
(Log(fluorescent units/area))
0.8
0.6
0.4
0.2
0.0
2.0
1.5
1.0
0.5
***
**
n.s.
N=167
N=222
N=152
N=195
N=175
N=221
N=155
N=261
0
30
Observation time (hours post exposure)

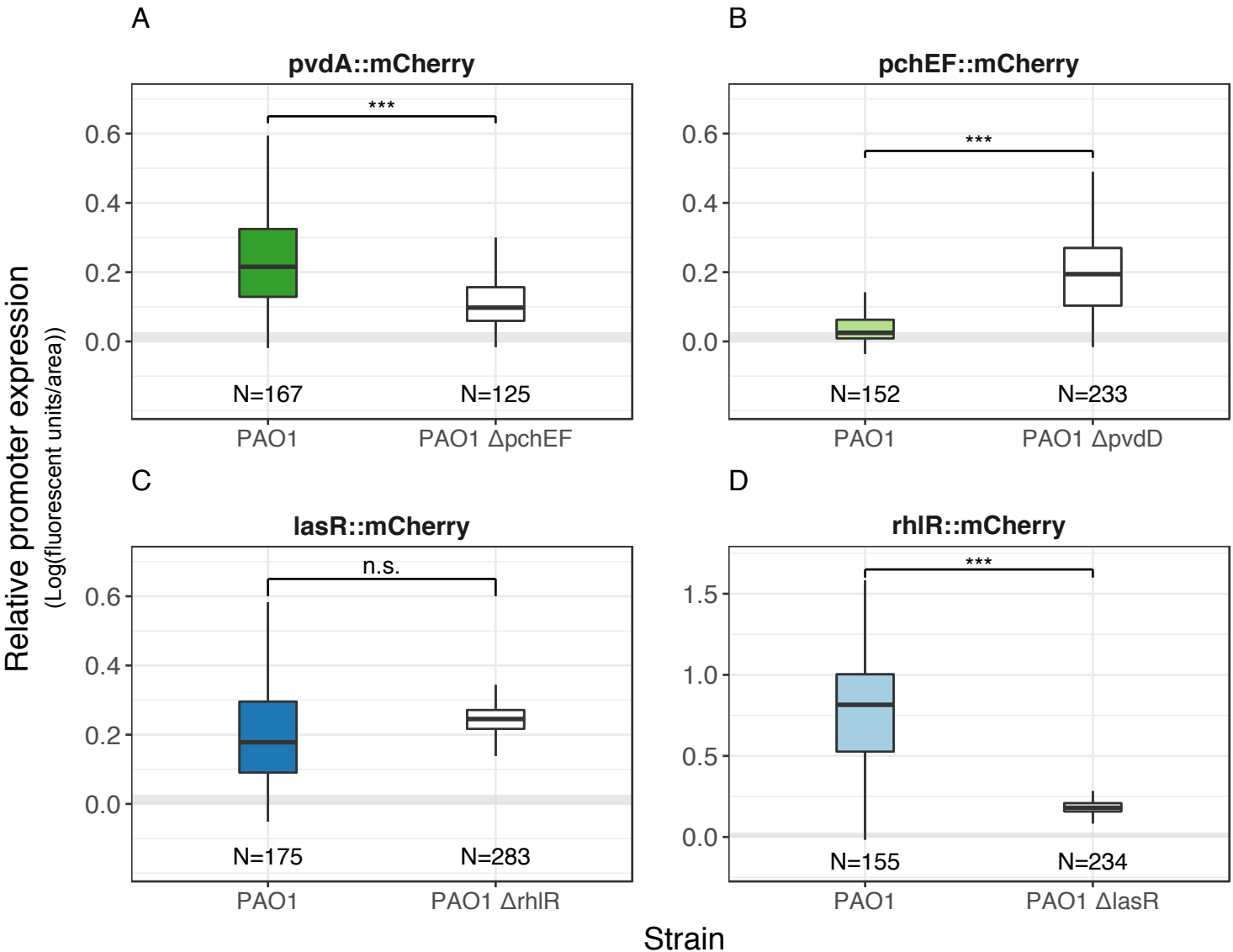
A
pvdA::mCherry
***
0.6
0.4
0.2
0.0
N=167
N=125
PAO1
PAO1 ΔpchEF
B
pchEF::mCherry
***
0.6
0.4
0.2
0.0
N=152
N=233
PAO1
PAO1 ΔpvdD
C
lasR::mCherry
n.s.
0.6
0.4
0.2
0.0
N=175
N=283
PAO1
PAO1 ΔrhlR
D
rhlR::mCherry
***
1.5
1.0
0.5
0.0
N=155
N=234
PAO1
PAO1 ΔlasR
Relative promoter expression
(Log(fluorescent units/area))
Strain

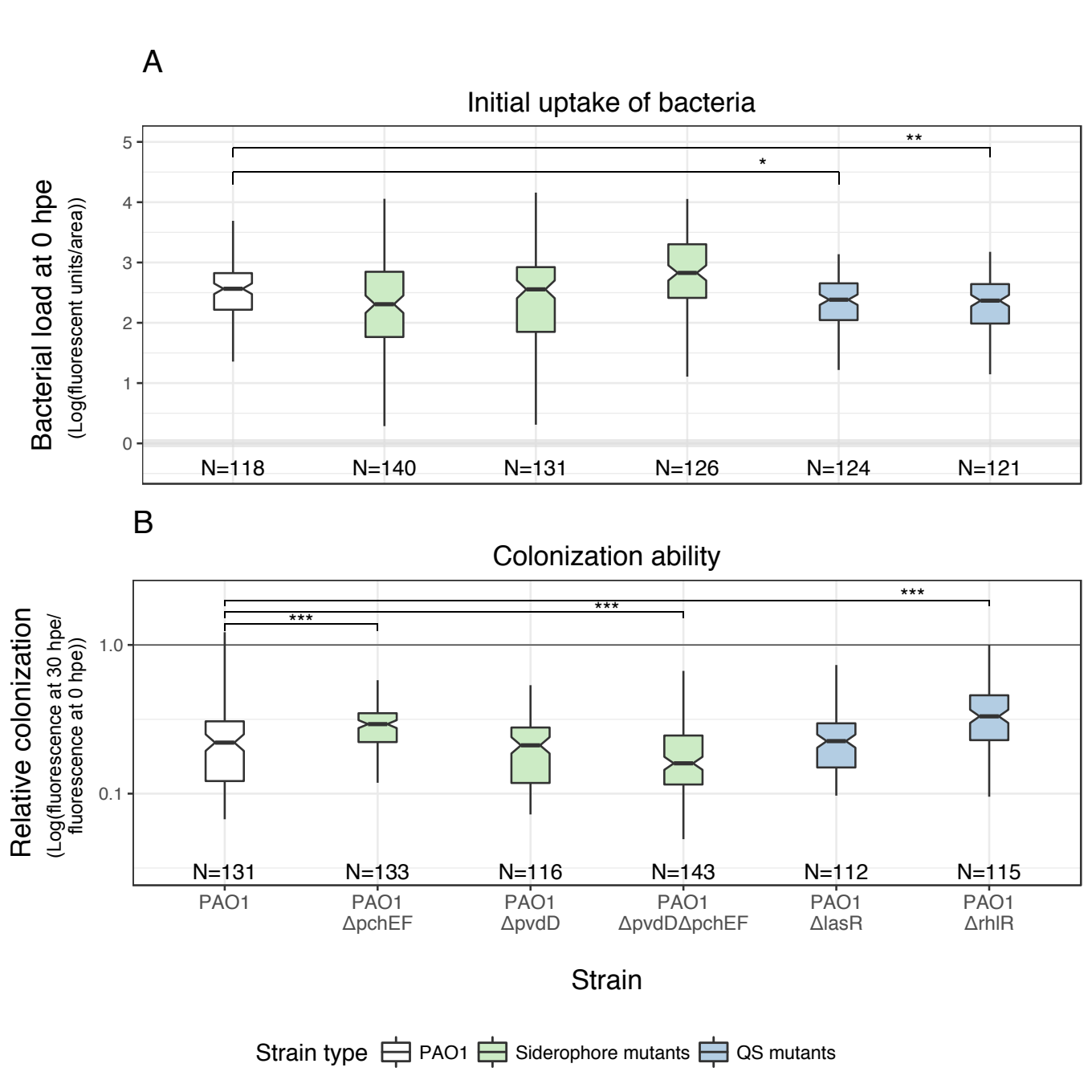
A
Initial uptake of bacteria
Bacterial load at 0 hpe
(Log(fluorescent units/area))
5
4
3
2
1
0
**
*
N=118
N=140
N=131
N=126
N=124
N=121
B
Colonization ability
Relative colonization
(Log(fluorescence at 30 hpe/
fluorescence at 0 hpe))
1.0
0.1
***
***
***
N=131
N=133
N=116
N=143
N=112
N=115
PAO1
PAO1
ΔpchEF
PAO1
ΔpvdD
PAO1
ΔpvdDΔpchEF
PAO1
ΔlasR
PAO1
ΔrhlR
Strain
Strain type
PAO1
Siderophore mutants
QS mutants

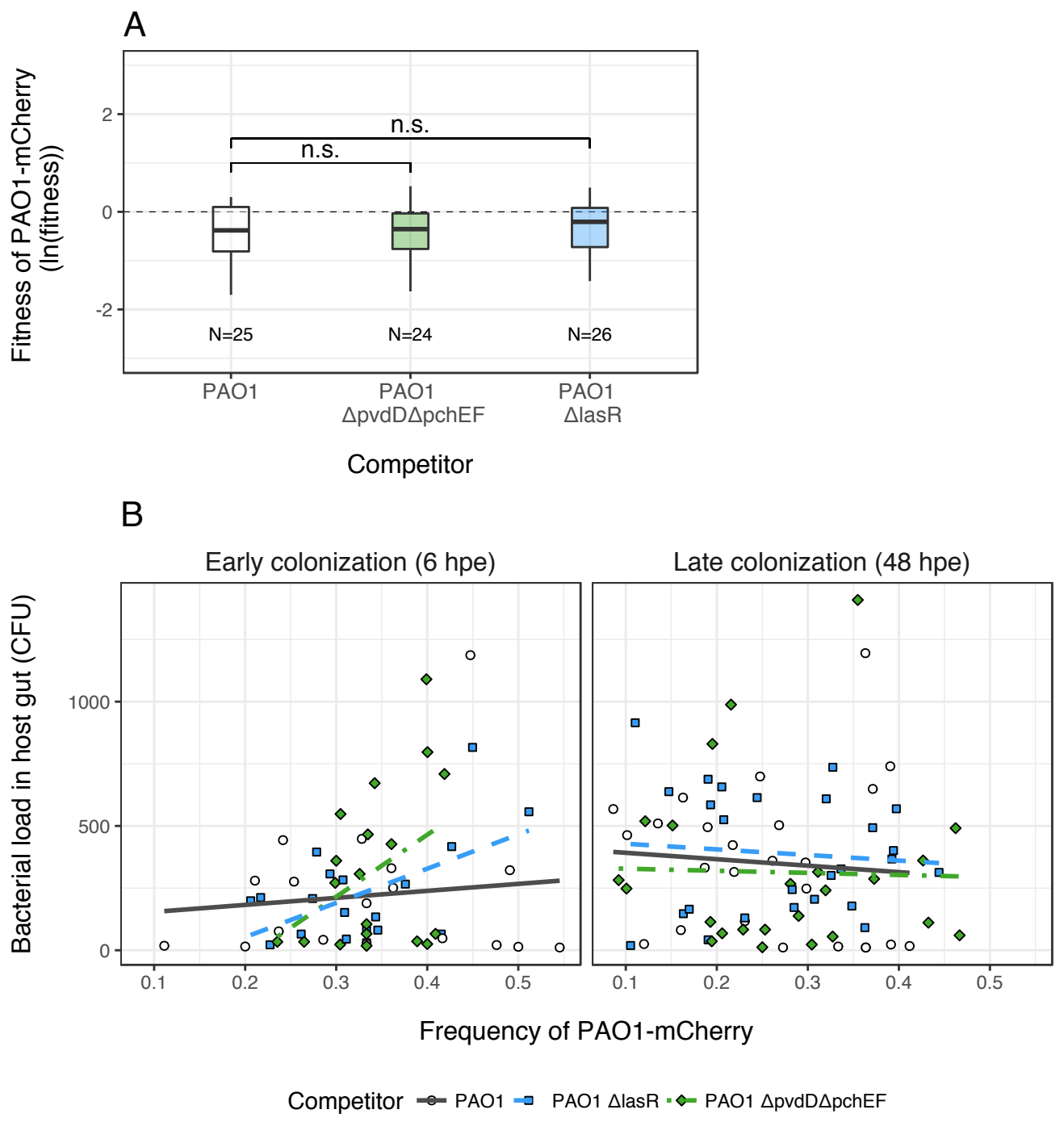
A
Fitness of PAO1-mCherry (ln(fitness))
2
0
-2
n.s.
n.s.
N=25
N=24
N=26
PAO1
PAO1 ΔpvdDΔpchEF
PAO1 ΔlasR
Competitor
B
Early colonization (6 hpe)
Late colonization (48 hpe)
Bacterial load in host gut (CFU)
1000
500
0
0.1
0.2
0.3
0.4
0.5
Frequency of PAO1-mCherry
Competitor
PAO1
PAO1 ΔlasR
PAO1 ΔpvdDΔpchEF

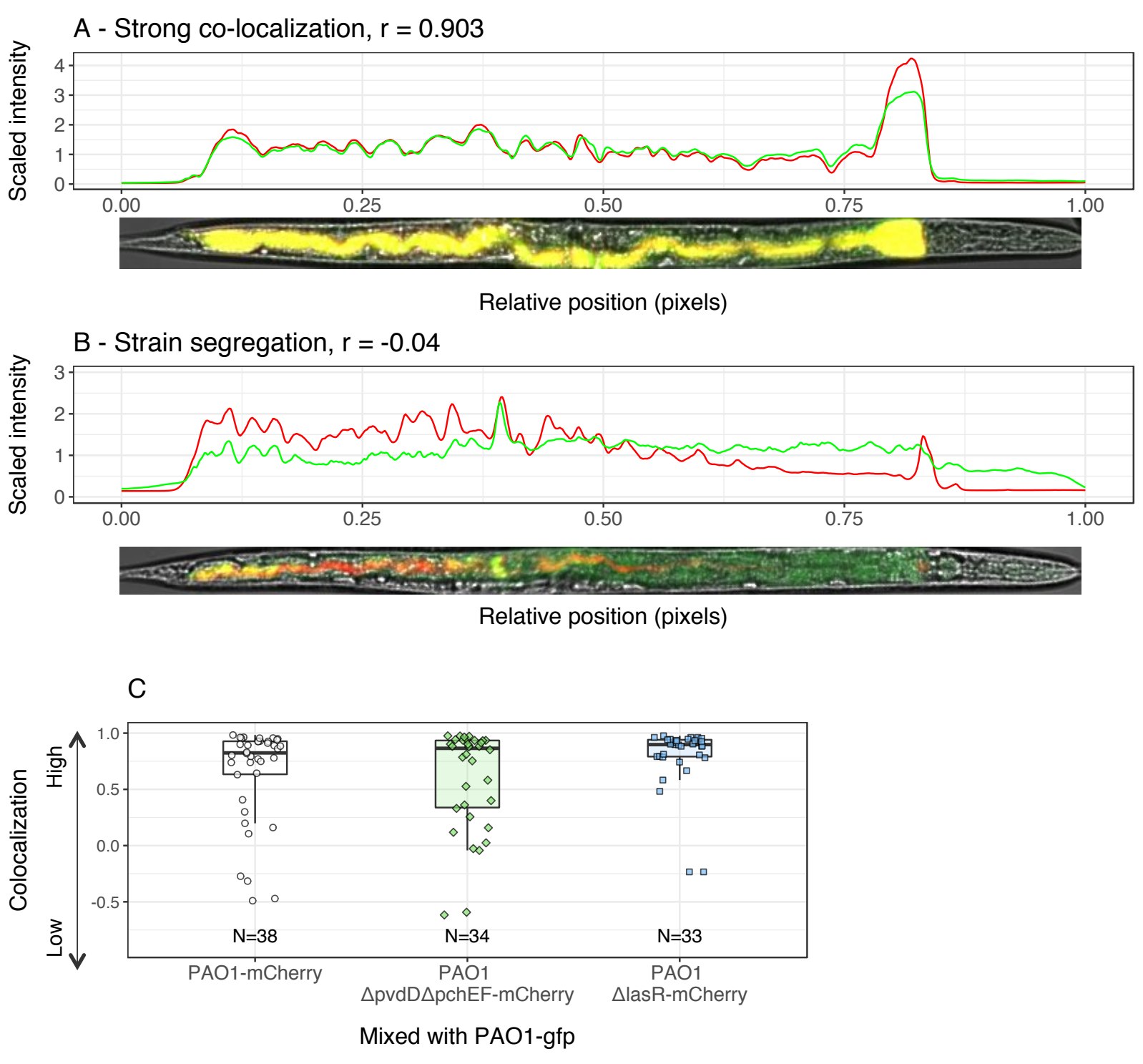
A - Strong co-localization, r = 0.903
Scaled intensity
4
3
2
1
0
0.00
0.25
0.50
0.75
1.00
Relative position (pixels)
B - Strain segregation, r = -0.04
Scaled intensity
3
2
1
0
0.00
0.25
0.50
0.75
1.00
Relative position (pixels)
C
Colocalization
High
Low
1.0
0.5
0.0
-0.5
N=38
N=34
N=33
PAO1-mCherry
PAO1 ΔpvdDΔpchEF-mCherry
PAO1 ΔlasR-mCherry
Mixed with PAO1-gfp